Institute of Physics Publishing Journal of Physics: Conference Series **16** (2005) 25–34
doi:10.1088/1742-6596/16/1/003 SciDAC 2005

Nonlinear extended magnetohydrodynamics simulation using high-order finite elements

C R Sovinec[1], D D Schnack[2], A Y Pankin[2], D P Brennan[3], H Tian[1], D C Barnes[4], S E Kruger[5], E D Held[6], C C Kim[1], X S Li[7], D K Kaushik[8], S C Jardin[9] and the NIMROD Team

[1]Engineering Physics Department, University of Wisconsin, Madison, WI 53706, USA
[2]Science Applications International Corporation, 10260 Campus Point Drive, San Diego, CA 92121, USA
[3]Laboratory for Nuclear Science, Massachusetts Institute of Technology, Cambridge, MA 02139, USA
[4]Center for Integrated Plasma Studies, University of Colorado, Boulder, CO 80309, USA
[5]Tech-X Corporation, 5621 Arapahoe Ave, Suite A, Boulder CO 80303, USA
[6]Physics Department, Utah State University, Logan, UT 84322, USA
[7]Lawrence Berkeley National Laboratory, One Cyclotron Road, Berkeley, CA 94720, USA
[8]Argonne National Laboratory, 9700 S. Cass Avenue, Argonne, IL 60439, USA
[9]Princeton Plasma Physics Laboratory, P.O. Box 451, Princeton, NJ 08543, USA

E-mail: sovinec@engr.wisc.edu

Abstract. Peak performance for magnetically confined fusion plasmas occurs near thresholds of instability for macroscopic modes that distort and possibly disrupt equilibrium conditions. In some cases, however, the best approach is to exceed stability thresholds and rely upon nonlinear saturation effects. Understanding this behaviour is essential for achieving ignition in future burning plasma experiments, and advances in large-scale numerical simulation have an important role. High-order finite elements permit accurate representation of extreme anisotropies associated with the magnetic field, and a new implicit algorithm has been developed for advancing the two-fluid model. Implementation of parallel direct methods for solving the sparse matrices makes the approach practical. The resulting performance improvements are presently being applied to investigate the evolution of 'edge localized modes' including important drift effects.

1. Introduction

Progress in the magnetic confinement of high-temperature plasmas has made it possible to realize self-sustained and controlled nuclear fusion in an experimental reactor. However, an improved understanding of dynamics in existing experiments and anticipating the behavior of future burning plasma experiments are critical for developing nuclear fusion as a commercially viable source of energy. To this end, large-scale numerical computation has an ever-increasing role in the theory of magnetized plasmas. The strong nonlinearities, competition among different physical effects, and

sensitivity to geometry are difficult or impossible to address analytically. All of these characteristics apply to the class of behavior labeled 'macroscopic.' Like the magnetohydrodynamics (MHD) of electrically conducting fluids, macroscopic plasma dynamics rearrange the magnetic-field configuration. They reduce the magnetic field's ability to contain and insulate the plasma from the surrounding material surfaces. While analytic theory has taught us what effects are important and how they can be described mathematically, understanding their consequences in specific experiments requires numerical computation.

Discovery of 'H-mode' operation [1] is one of the most important advances in magnetic confinement. Sheared plasma flow forms a barrier to cross-field transport near the edge of the closed magnetic flux region. This leads to locally strong gradients in number density and pressure, which significantly boost the ratio of stored thermal energy to magnetic confinement energy for the entire configuration. However, the strong gradients also lead to edge localized modes (ELMs), which allow energy transport across the barrier in periodic events. When scaled to reactor conditions, 'Type-I' ELMs are expected to be strong enough to cause significant material damage to the first wall. Understanding and controlling this form of macroscopic activity is therefore particularly important at this time.

Recent theoretical work has shown that H-mode equilibria are linearly unstable to MHD modes that are driven by a combination of the localized pressure gradient and the associated charge current density profile [2]. Numerical computations have been applied to show how the linear properties are related to other MHD modes and how the behavior changes with equilibrium parameters and wavelength [3]. The linear spectrum is very broad, however, and large-scale nonlinear simulation is required to determine how the MHD instability leads to the bursting transport events observed in experiment. The first series of such simulations [4] solves a system of equations that models important drift effects associated with the finite size of charged-particle gyro-orbits but not fast compressional effects. Preliminary nonlinear simulations with a more complete geometrical representation have also been performed—with the simpler physics model of compressible MHD. Ultimately, simulations with full geometry, drift effects, and kinetic effects are needed.

In this article, we describe computational advances that have been made for the NIMROD (Non-ideal MHD with Rotation, Open Discussion) code [5] under the auspices of the SciDAC program to address ELMs and other macroscopic activity. We begin section 2 with a description of the spatial representation that permits accurate computation of the extreme anisotropies of magnetized plasmas in full geometry calculations. We then consider the numerical time-advance, highlighting developments for drift effects and the approach for solving the resulting algebraic systems. Section 3 describes preliminary ELM calculations that include drift effects and fast waves, and section 4 has concluding remarks.

2. Computational developments for macroscopic modelling

Macroscopic dynamics in magnetized plasmas occur over time-scales that are short compared to the duration of an experiment but long relative to the propagation of plasma waves that communicate perturbations globally. Implicit methods are, therefore, essential for solving initial-value problems. They are also practical [6-8] for fluid-based models, the MHD and two-fluid (electron-ion) models. They are systems of nonlinear partial differential equations (PDEs) that describe the evolution of low-order velocity moments of particle distribution functions. At relatively low temperature where the plasma is collisional, the fluid description is comprehensive [9]. For high-temperature plasmas, non-local kinetic effects can be added through closure relations that make the system integro-differential [10].

2.1. Spatial representation

Magnetic confinement configurations are typically toroidal in shape to avoid the end losses associated with open systems. The geometry and equilibrium state in the tokamak and several other devices have toroidal symmetry, but the poloidal cross-section may be irregular. The NIMROD code has been developed for these configurations and uses finite elements for the poloidal plane and finite Fourier series for toroidal direction. The highest spatial derivatives in the PDE system for the primitive

physical fields [plasma flow velocity (**V**), magnetic field (**B**), particle number density (n), and species temperatures (T_i and T_e for ions and electrons)] result from collisional effects and are second-order. While the system has a hyperbolic character associated with the propagation of waves, resolving the effects of the second-order terms is usually necessary for the macroscopic dynamics that affect the magnetic configuration. A conforming finite element representation then requires a polynomial basis where first-derivatives are square-integrable [11]. (Formulation in terms of scalar potential fields can be accomplished using a basis with continuous derivates—see reference [12].) For the MHD model, an effective semi-implicit algorithm applies self-adjoint differential operators at the advanced time-level, so its weak form constitutes a sequence of variational problems. Adding drift effects breaks this mathematical symmetry, and the weak form is not variational.

The NIMROD code was the first to use high-order two-dimensional finite elements in application to nonlinear fusion plasma dynamics. The implementation allows the user to select basis functions of any degree from the classes of Lagrange and Gauss-Lobatto-Legendre polynomials. As described in reference [5], we have found the high-order finite element representation to be beneficial in several respects. First, divergence errors in the computed magnetic field can be made small—a finding which is consistent with analysis (see [13] and references therein) performed for incompressible fluid computations. Second, it is possible to resolve the extremely anisotropic properties of magnetized plasmas without significant alignment of the magnetic field and the mesh. Third, nonuniform meshing does not upset high-order convergence properties, and the boundary condition treatment does not change with the degree of the polynomial basis functions. Fourth, using isoparametric mappings from element coordinates to physical space [11] provides an efficient means for representing the curved geometry of the equilibrium state. The results from a resistive MHD benchmark illustrate the effectiveness of the high-order representation with a packed mesh of curved finite elements. The anisotropic nature of the Lorentz force and the resonance condition for the wavenumber vector of the helical perturbation and the equilibrium magnetic field, $\mathbf{k} \cdot \mathbf{B}_0 = 0$, lead to the localization shown in figure 1, and convergence of the magnetic-field solution with different basis functions is shown in figure 2. Tests demonstrating the effectiveness on extremely anisotropic thermal conduction are detailed in reference [5].

The spatial representation also affects the manner in which kinetic effects of the electrons and majority ions are incorporated into the modelling. Effects associated with charged particles rapidly streaming along magnetic field-lines are computed through solutions of a drift kinetic equation using the method of characteristics and a basis function expansion in velocity space [10]. The finite element/finite Fourier series spatial representation provides a meaningful prescription of the fields that influence the kinetic distortions along the characteristic trajectories. The parallel heat flux and parallel stress are determined at the nodes of the finite element mesh and interpreted with the respective basis functions as closure information in the fluid model. In some cases, important effects also arise from a minority species of high-temperature ions—fusion products or ions that have been inserted via neutral beams. The M3D group has proven the effectiveness of combining particle-in-cell methods with finite elements for this purpose [7], and the NIMROD effort has extended this for high-order elements [14]. Though accumulating characteristic information into a closure relation is common to both types of numerical kinetics, the particle approach relies on statistics to resolve velocity-space variations instead of basis function expansions. (The finite element/finite Fourier series spatial representation is used in all of the fluid and kinetic models.) When including the hot-particle effects, we find a significant reduction in simulation-particle noise by integrating the kinetic-stress term by parts.

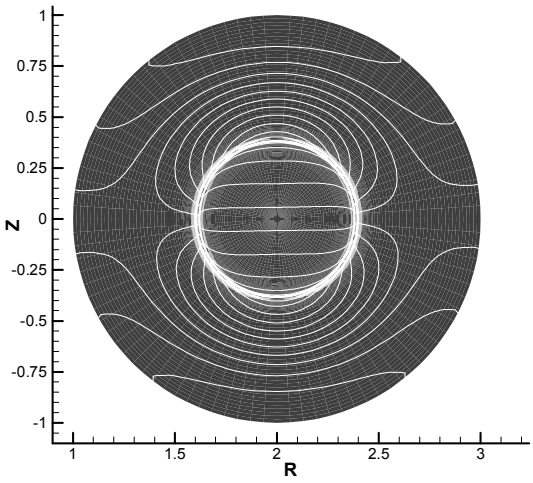

Figure 1. Cylindrical benchmark results illustrating localization of out-of-plane flow amplitude (lighting intensity) and out-of-plane magnetic field (contour lines) for a helical MHD tearing mode. The mesh is 24×24 (radial-azimuthal) curved biquartic elements, packed in the radial direction.

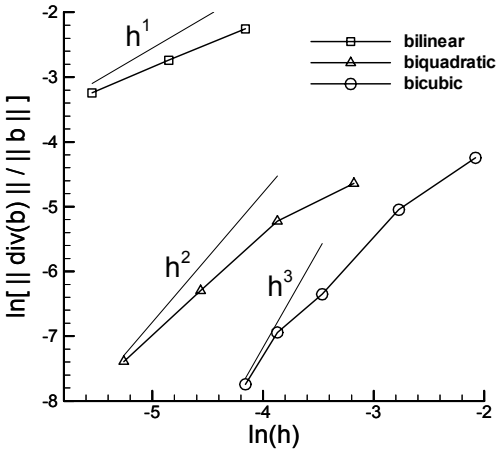

Figure 2. Convergence studies on the magnetic divergence constraint for the cylindrical benchmark calculation with bilinear, biquadratic, and bicubic finite elements (from [5]). The parameter h is the inverse of the number of elements in each direction, and the convergence rates expected from analysis (for first derivatives of the solution) are illustrated.

2.2. Time-advance

An important physical consideration for the time-advance is that resistive and viscous dissipation are small in high-temperature plasmas, but they must be treated accurately to reproduce the macroscopic behaviour that changes magnetic topology. Fortunately, the dynamics of interest does not include shock propagation, and methods that introduce numerical dispersion to stabilize wave propagation at large time-step are suitable. For nonlinear resistive MHD, we are able to adapt a semi-implicit method [6] that had previously been used with a finite-volume spatial representation. It is based on the leapfrog method for wave propagation and includes a positive-definite self-adjoint differential operator with a coefficient that scales as $c^2\Delta t^2$, where c is a characteristic wave speed and Δt is the time-step. The spectrum of this operator governs temporal convergence in multi-scale computations [6]. An additional benefit when using a finite element spatial representation is that the anisotropic operator which distinguishes the fast, shear, and slow modes of the MHD spectrum [15] is straightforward to implement and, by construction, results in a Hermitian matrix for the velocity advance [5]. For the subdominant plasma flow, advective terms can be treated with predictor-corrector steps [16].

As their name implies, plasma drift effects induce propagation, and they alter the stability of MHD modes. In addition, two-fluid models have important dispersive waves, where frequencies are related to the square of the wavenumber, $\omega \sim k^2$. These properties change the mathematical character of the PDE system, and (contrary to reference [17]), we have not found it practicable to retain only self-adjoint operators for large-Δt stabilization. One possibility is to use a time-centred implicit method [12,18]. Another method that is being analysed and implemented retains the staggered differencing between $\mathbf{V}$ and other fields in the time domain and uses implicit operators at each step. Terms associated with drift and dispersive waves are made numerically stable by non-self-adjoint differential operators, while the operator for MHD waves is unchanged. Taking the limit of zero electron mass, the staggered time-discrete form of the two-fluid model with drift effects is:

$$m_{\rm i} n^{j+1/2}\left(\frac{\Delta\mathbf{V}}{\Delta t}+\frac{1}{2}\mathbf{V}^{j}\cdot\nabla\Delta\mathbf{V}+\frac{1}{2}\Delta\mathbf{V}\cdot\nabla\mathbf{V}^{j}\right)-\Delta t L^{j+1/2}\left(\Delta\mathbf{V}\right)+\nabla\cdot\Pi_{\rm i}\left(\Delta\mathbf{V}\right)=\mathbf{J}^{j+1/2}\times\mathbf{B}^{j+1/2}$$
$$-m_{\rm i} n^{j+1/2}\mathbf{V}^{j}\cdot\nabla\mathbf{V}^{j}-\nabla p^{j+1/2}-\nabla\cdot\Pi_{\rm i}\left(\mathbf{V}^{j}\right) \tag{1}$$

$$\frac{\Delta n}{\Delta t}+\frac{1}{2}\mathbf{V}^{j+1}\cdot\nabla\Delta n=-\nabla\cdot\left(\mathbf{V}^{j+1}\cdot n^{j+1/2}\right) \tag{2}$$

$$\frac{3n}{2}\left(\frac{\Delta T_\alpha}{\Delta t}+\frac{1}{2}\mathbf{V}_\alpha^{j+1}\cdot\nabla\Delta T_\alpha\right)+\frac{1}{2}\nabla\cdot\mathbf{q}_\alpha\left(\Delta T_\alpha\right)=-\frac{3n}{2}\mathbf{V}_\alpha^{j+1}\cdot\nabla T_\alpha^{j+1/2}-nT_\alpha^{j+1/2}\nabla\cdot\mathbf{V}_\alpha^{j+1}$$
$$-\nabla\cdot\mathbf{q}_\alpha\left(T_\alpha^{j+1/2}\right)+Q_\alpha^{j+1/2} \tag{3}$$

$$\frac{\Delta\mathbf{B}}{\Delta t}+\frac{1}{2}\mathbf{V}^{j+1}\cdot\nabla\Delta\mathbf{B}+\frac{1}{2}\nabla\times\frac{1}{ne}\left(\mathbf{J}^{j+1/2}\times\Delta\mathbf{B}+\Delta\mathbf{J}\times\mathbf{B}^{j+1/2}\right)+\frac{1}{2}\nabla\times\eta\Delta\mathbf{J}$$
$$=-\nabla\times\left[\frac{1}{ne}\left(\mathbf{J}^{j+1/2}\times\mathbf{B}^{j+1/2}-\nabla p_{\rm e}\right)-\mathbf{V}^{j+1}\times\mathbf{B}^{j+1/2}+\eta\mathbf{J}^{j+1/2}\right] \tag{4}$$

where superscripts show the time-level indices, and Δ indicates the change from a single step. The charge current density is directly related to magnetic field, $\mu_0\mathbf{J}=\nabla\times\mathbf{B}$, the number density is the same for the two species (α=i,e), and $m_{\rm i}$ is the ion mass. The ion flow velocity ($\mathbf{V}_{\rm i}$) is equivalent to the plasma flow velocity, while the electron flow velocity is $\mathbf{V}_{\rm e}=\mathbf{V}-\mathbf{J}/ne$. The pressure p (without subscript) is the sum of the electron and ion pressures, $n\left(T_{\rm e}+T_{\rm i}\right)$, and the differential operator L in (1) is the linear MHD force operator,

$$L\left(\Delta\mathbf{V}\right)=\frac{1}{\mu_0}\left\{\nabla\times\left[\nabla\times\left(\Delta\mathbf{V}\times\mathbf{B}\right)\right]\right\}\times\mathbf{B}+\mathbf{J}\times\nabla\times\left(\Delta\mathbf{V}\times\mathbf{B}\right)+\nabla\left(\Delta\mathbf{V}\cdot\nabla p+\frac{5}{3}p\nabla\cdot\Delta\mathbf{V}\right).$$

Heating in (3) for each species appears as the term Q_α, and η is the electrical resistivity. The number density appearing in (3) and (4), may be averaged from the j+1/2 and j+3/2 time-levels, since both values are available. However, the j+1 level of electron flow in the electron temperature advance is not known until after the magnetic advance, so (3) may be solved first without the updated $\mathbf{V}_{\rm e}$ to predict $p_{\rm e}$ for (4), followed by a correction of electron temperature with the updated $\mathbf{V}_{\rm e}$.

Important drift effects from finite-sized gyro-orbits appear in (1), (3), and (4). In the flow velocity evolution (1), they result from the gyroviscous part of the traceless stress tensor, $\Pi_{\rm i}$, and for the Braginskii model [9], the gyroviscous stress is

$$\Pi_{\rm gv}=\frac{m_{\rm i}p_{\rm i}}{4eB}\left[\hat{\mathbf{b}}\times\mathbf{W}\cdot\left(\mathbf{I}+3\hat{\mathbf{b}}\hat{\mathbf{b}}\right)-\left(\mathbf{I}+3\hat{\mathbf{b}}\hat{\mathbf{b}}\right)\cdot\mathbf{W}\times\hat{\mathbf{b}}\right],\qquad\left(\mathbf{W}\equiv\nabla\mathbf{V}+\nabla\mathbf{V}^{\rm T}-\frac{2}{3}\mathbf{I}\nabla\cdot\mathbf{V}\right)$$

where $\hat{\mathbf{b}}\equiv\mathbf{B}/B$. The heat flux vectors $\mathbf{q}_\alpha$ for separate species temperatures contain a term that directs heat perpendicular to both the magnetic field and the temperature gradient, $+2.5p_{\rm i}\left(eB\right)^{-1}\hat{\mathbf{b}}\times\nabla T_{\rm i}$ for ions and $-2.5p_{\rm e}\left(eB\right)^{-1}\hat{\mathbf{b}}\times\nabla T_{\rm e}$ for electrons. In (4), the terms associated with drifts appear explicitly. Finite ion pressure leads to an imbalance between the Lorentz force and the electron pressure gradient, which causes magnetic perturbations to drift.

To ensure that the algorithm is numerically stable, the drift terms are being implemented implicitly, as indicated in (1)-(4). Unlike the MHD algorithm [5], the differential operators acting on the time-advanced fields are not self-adjoint. This has practical consequences, but once addressed, there is no additional computational penalty in making the advective terms implicit. The stability of our semi-

implicit method for MHD with implicit advection has already been demonstrated [19], and numerical analysis shows that implicit advection is compatible with the two-fluid leapfrog algorithm.

2.3. Computing solutions

There are three general aspects to solving the two-fluid model with the time-advance shown in (1)-(4) and the finite element/finite Fourier series spatial representation. First, numerical quadrature is used to perform the volume integrals required by the weak form of the equations, and this involves gather/scatter operations. Second, Fast Fourier Transforms (FFTs) are applied to evaluate terms that couple Fourier components in nonlinear simulations, thereby avoiding convolution operations. Third, and most important for computational performance, the algebraic systems in (1)-(4) resulting from the implicit temporal differencing have to be solved at every time-step, and even with the implicit approach, tens of thousands of time-steps may be needed during a nonlinear simulation.

For linear calculations, the assumed toroidal symmetry of the bounding wall and equilibrium makes the toroidal angle an ignorable coordinate. There is no coupling among toroidal Fourier harmonics, and the algebraic systems represent interaction across the nodes of the finite element mesh only. The matrices are sparse (see figure 3), and elements are computed from the weak form of the system. In some three-dimensional nonlinear MHD simulations, coefficients of the implicit terms can be approximated with their toroidally averaged values. While coupling among Fourier components results from terms on the right sides of (1)-(4), the algebraic system for each Fourier component is solved independently with partitioned parallel communication. Since the matrix elements are known, static condensation is used to reduce the size of the system by eliminating coefficients for element interior nodes in terms of other coefficients. With biquartic elements, for example, the system size is reduced by more than a factor of two. Nonetheless, the matrices are ill-conditioned. With the time-step equal to the Alfvén-wave propagation time, even a modest version of the computation shown in figure 1 (with a 12×12 mesh of packed biquartic elements) needs to solve a matrix with a condition number of 23,000, which is an order of magnitude larger than the condition number of the corresponding discrete vector Laplacian operator, during each time-step. Condition numbers are much larger in production simulations, where five or more times as many elements may be used in each of the poloidal directions.

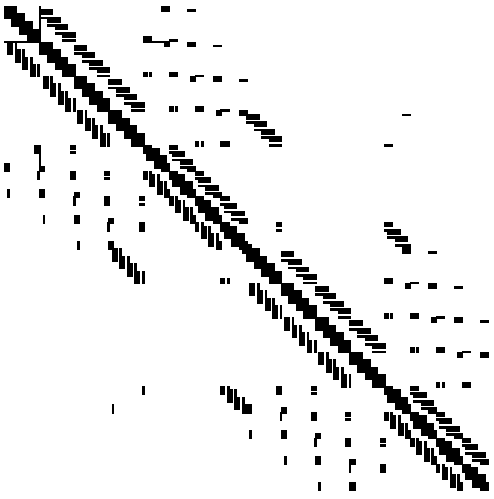

Figure 3. Matrix sparsity pattern resulting from a small (8×8) polar mesh of biquartic elements after static condensation but before reordering. The node ordering is influenced by domain decomposition for parallel computation. Here, the mesh is evenly decomposed into four subdomains.

Applying the SuperLU parallel solver library [20] to solve the ill-conditioned matrices leads to significant improvement in NIMROD's computational performance on the MHD system. Developed for sparse matrices, SuperLU allows reordering to minimize bandwidth before factoring, and once factored, its direct method solves the ill-conditioned systems to the necessary tolerance in far less time than preconditioned Krylov methods. With SuperLU, NIMROD completes linear MHD calculations more than 100 times faster than with the conjugate gradient method using global line-Jacobi preconditioning. Nonlinear simulations also benefit very significantly; the factor of five shown in figure 4 is typical. Although re-factoring for a direct solve can be costly, matrix elements and factors are saved and reused until they change beyond a prescribed tolerance. For nonlinear simulations where the coefficients of implicit terms develop important toroidal variations, it is not practical to find the matrix elements that represent convolutions of Fourier components. The direct solver is then used in combination with a matrix-free Krylov method, which performs FFTs as part of the computation of the full matrix-vector product. SuperLU is applied to the parts of the system without Fourier component coupling as an effective preconditioning step.

The SuperLU library is also facilitating our implementation of the time-advance for the two-fluid system. The solvers are applicable to the non-symmetric matrices that arise from the implicit drift and advection terms. At the time of writing, a matrix-free solve for non-symmetric systems is needed for full nonlinear simulation capability. We anticipate use of direct solves for preconditioning, similar to what has been successful for the matrix-free solves of symmetric systems.

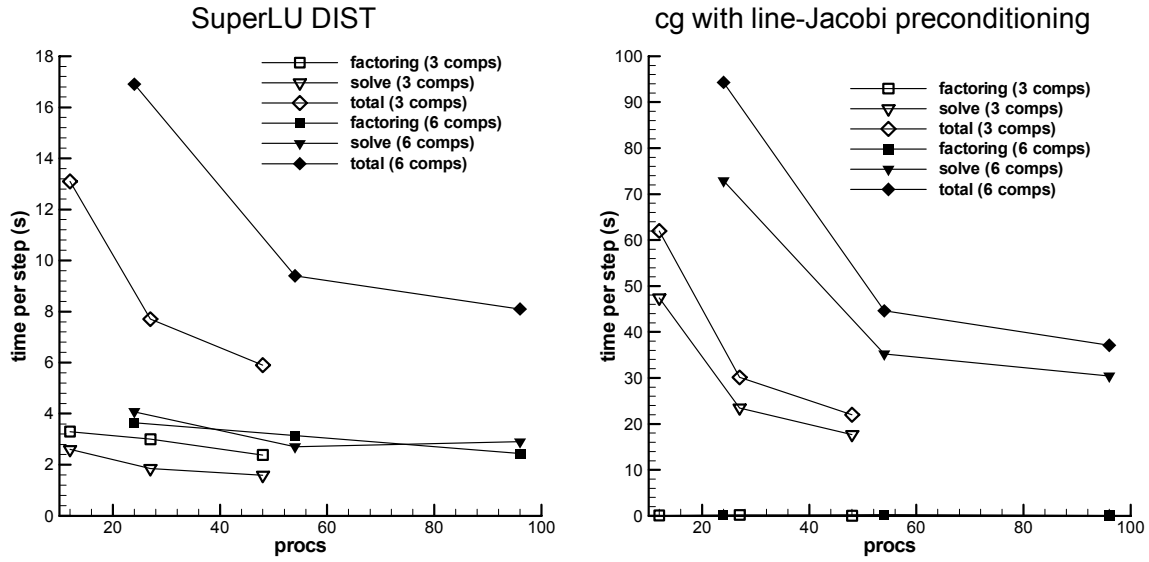

Figure 4. Comparison of parallel scaling performance with the SuperLU DIST library shown on the left and with the preconditioned conjugate gradient method on the right. The nonlinear computation has a 32×32 mesh of biquartic finite elements, and the number of toroidal Fourier harmonics are indicated for different cases in the plots. On average, the matrices and factors are recreated every eight time-steps, and the timings are taken from an IBM SP3.

3. Application to edge localized modes

The linear modes underlying ELM activity are unstable in the ideal MHD model, which means that magnetic topology change is not required to release free energy. The growth rates can approach Alfvén-wave propagation rates, so the mathematical system does not have the extreme stiffness of the applications to slower collision-dependent dynamics. Nonetheless, there is a range of temporal scales, particularly with the two-fluid model, and perturbations are active in the large equilibrium gradient near the edge of the confinement region (figure 5a). We therefore take advantage of the finite element representation by concentrating the mesh to resolve the region of interest with biquartic elements and

an isoparametric mapping (figure 5b) that approximates the shape of the equilibrium distribution. At the low temperatures found outside the pressure gradient, the electrical resistivity of the plasma is relatively high. For linear computations, the resistivity has a fixed profile. However, nonlinear simulations rely upon temperature-dependent resistivity and anisotropic thermal conduction [8] to distinguish the response of plasma on the two sides of the magnetic separatrix that defines the edge of the confinement region.

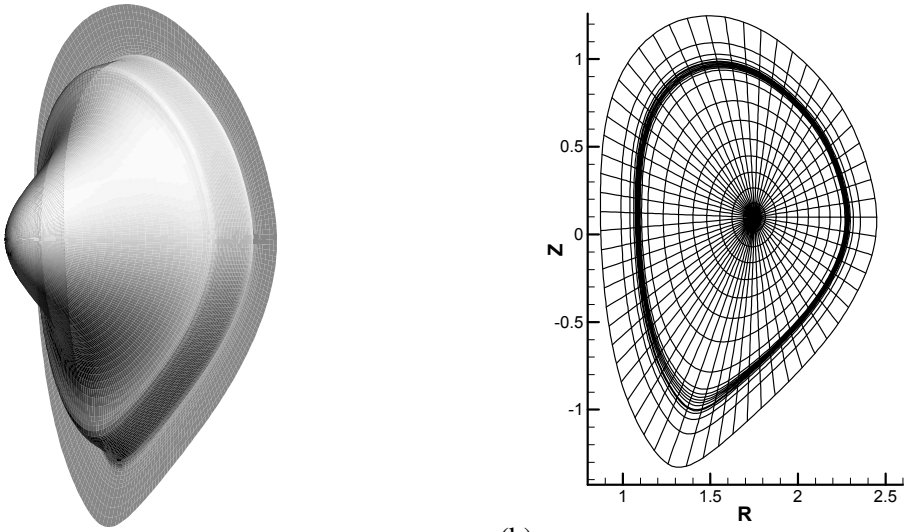

(a) (b)

Figure 5. Pressure distribution in the shaped toroidal equilibrium that is unstable to ELMs (a) and a 20×60 mesh of biquartic finite elements with mesh packing near the edge pressure gradient (b).

Preliminary nonlinear simulations of ELMs using the resistive MHD model demonstrate the feasibility of full-geometry computations. However, drift effects are known to be stabilizing for modes with large wavenumber [21], and without these effects, the nonlinear simulations cannot achieve resolution in the toroidal direction. Fluctuation energy tends to accumulate at the highest toroidal harmonics retained in a computation if an artificial damping term is not added.

As a step toward full nonlinear ELM simulations with drift effects, we are now running linear calculations with the two-fluid system. Figure 6 compares pressure perturbations from the MHD model with a two-fluid calculation that includes drift effects in the magnetic field evolution and in the flow velocity evolution through the gyroviscous term. The peak amplitude of this n=40 mode (where n is the toroidal harmonic number) shifts downward from the outermost extent of the confinement region. There is a modest drop in growth rate from $\gamma\tau_A$=0.62 to $\gamma\tau_A$=0.53, and the mode acquires a finite real frequency of 0.07 τ_A^{-1}. The mode structure is well resolved with the 20×90 mesh of biquartic elements, but the results need to be confirmed with thermal drift effects and the ion flow profile that is consistent with the equilibrium data.

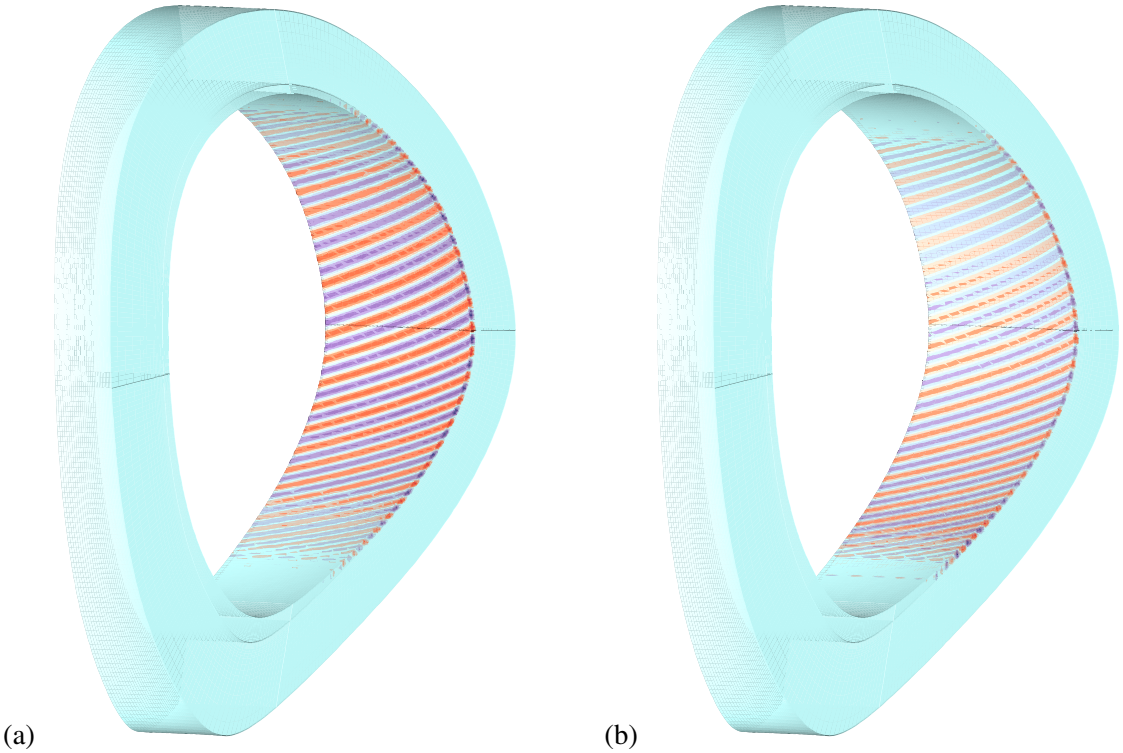

(a) (b)

Figure 6. Mode structure of an unstable ELM in the MHD model (a) and in the two-fluid model including drift effects through the Hall term in the magnetic evolution and through gyroviscosity in the flow velocity advance (b). One-sixteenth of the torus is shown, and the confined-plasma region is removed from the plots to expose the mode structure.

4. Conclusions

Understanding and control of the evolution of ELMs is one of the most important scientific issues for a large burning plasma experiment, so we have highlighted the NIMROD simulation effort in this area. Nonetheless, the modelling development supported by the SciDAC program is being applied to a range of macroscopic activity in a number of laboratory devices [8]. It is also being applied to study possible relaxation effects in astrophysical jets. Solving the stiff nonlinear PDE systems resulting from fluid-based plasma models requires advanced mathematical and computational techniques. High-order finite elements prove extremely useful for resolving extreme anisotropies and for minimizing magnetic divergence error, and a new implicit time-advance has been developed for the two-fluid model with drift effects. Practical application of these methods has been made possible through the SuperLU library, which addresses sparse matrices with reordering and factorisation. It is used as both a solver for matrices with readily computed elements and as a preconditioner for matrices that contain spectral convolutions.

Acknowledgments

The authors wish to thank the M3D developers (the NIMROD Team's sister group in the Center for Extended Magnetohydrodynamics) for valuable discussions and benchmarking. This work is supported by the U.S. Department of Energy through the Center for Extended Magnetohydrodynamics and the Terascale Optimal PDE Simulation Center under the auspices of the SciDAC program. Simulations have been performed using resources of the National Energy Research Scientific Computing Center.

References

[1] Wagner F *et al.* 1982 *Phys. Rev. Lett.* **49** 1408
[2] Connor J W, Hastie R J, Wilson H R and Miller R L 1998 *Phys. Plasmas* **5** 2687
[3] Snyder P B, Wilson H R, Ferron J R, Lao L L, Leonard A, Osborne T H, Turnbull A D, Mossessian D, Murakami M and Xu X Q 2002 *Phys. Plasmas* **9** 2037
[4] Snyder P B, Wilson H R and Xu X Q 2005 *Phys. Plasmas* **12** 056115
[5] Sovinec C R, Glasser A H, Gianakon T A, Barnes D C, Nebel R A, Kruger S E, Schnack D D, Plimpton S J, Tarditi A, Chu M S and the NIMROD Team 2004 *J. Comput. Phys.* **195** 355
[6] Schnack D D, Barnes D C, Miki Z, Harned D S and Caramana E J 1987 *J. Comput. Phys.* **70** 330
[7] Park W, Belova E V, Fu G Y, Tang X Z, Strauss H R and Sugiyama L 1999 *Phys. Plasmas* **6** 1796
[8] Sovinec C R, Gianakon T A, Held E D, Kruger S E, Schnack D D and the NIMROD Team 2003 *Phys. Plasmas* **10** 1727
[9] Braginskii S I 1965 Transport processes in a plasma *Reviews of Plasma Physics* vol 1 ed M Leontovich (New York: Consultants Bureau) p 205
[10] Held E D, Callen J D, Hegna C C, Sovinec C R, Gianakon T A and Kruger S E 2004 *Phys. Plasmas* **11** 2419
[11] Strang G and Fix G J 1973 *An analysis of the finite element method* (Englewood Cliffs NJ: Prentice-Hall)
[12] Jardin S C and Breslau J A 2005 *Phys. Plasmas* **12** 056101
[13] Gunzburger M D 1988 Mathematical aspects of finite element methods for incompressible viscous flows *Finite Element Thoery and Application: Proc. ICASE Finite Element Thoery and Application Workshop (Hampton, Virginia 28-30 July 1986)* ed D L Dwoyer, M Y Hussaini and R G Voigt (New York: Springer-Verlag) pp 124-150
[14] Kim C C, Sovinec C R, Parker S E and the NIMROD Team 2004 *Comput. Phys. Comm.* **164** 448
[15] Lerbinger K and Luciani J F 1991 *J. Comput. Phys.* **97** 444
[16] Lionello R, Miki Z and Linker J A 1999 *J. Comput. Phys.* **152** 346
[17] Harned D S and Miki Z 1989 *J. Comput. Phys.* **83** 1
[18] Chacón L and Knoll D A 2003 *J. Comput. Phys.* **188** 573
Barnes D C 2004 *Bull. Am. Phys. Soc.* **49** no 8 p 183
[19] Sovinec C R and the NIMROD Team 2003 *Bull. Am. Phys. Soc.* **48** no 7 p 115
[20] Li X S and Demmel J W 2003 *ACM Trans. Math. Software* **29** 110
[21] Rogers B N and Drake J F 1999 *Phys. Plasmas* **6** 2797